Available online at www.sciencedirect.com
ScienceDirect
Journal of Sound and Vibration 310 (2008) 527–540
JOURNAL OF SOUND AND VIBRATION
www.elsevier.com/locate/jsvi

Surface perturbation technique for flow-induced vibration and noise control

L. Cheng*, Y. Zhou

Department of Mechanical Engineering, The Hong Kong Polytechnic University, Hung Hom, Kowloon, Hong Kong

Received 18 December 2006; received in revised form 5 October 2007; accepted 5 October 2007
Available online 8 November 2007

Abstract

A novel surface perturbation technique has been developed recently and applied to control fluid–structure interactions, including vortex streets, flow-induced vibrations and vortex-induced noise. In this article, we summarize this technique, major applications, control performances, and possible physical mechanisms responsible for flow modification, drag reduction, controlling fluctuating forces/structural vibrations, and noise control.

1. Introduction

Fluid–structure interactions are widely seen in engineering. For example, when flow blows over a slender structure (off-shore structures, high-rise buildings, cable-stayed bridges, and fluid machinery, etc.), vortices separate alternately from the structure, giving rise to excitation forces and causing the structure to vibrate [1]. The structural motion in turn influences the flow field, resulting in a highly nonlinear fluid–structure coupling [2,3]. This type of fluid–structure interaction may affect the fatigue life of engineering structures and even lead to structural damages and serious accidents, and has become one of the major concern in many applications. Furthermore, vortex shedding is responsible for noise generation in case the kinetic energies of vortical motions are converted into the acoustic wave involving the longitudinal oscillation of fluid particles [4]. Therefore, the control of flow and its induced structural vibration has attracted the interests of many researchers for many years.

A variety of control techniques have been developed in the past, and may be passive and active. The passive technique requires no external energy, producing desired effects on flow by changing structural geometries, adding grooves, shrouds or near-wake stabilizers to structures [5,6]. The active technique involves energy input via the use of actuators to bring about desirable changes to the fluid–structure system using either an independent external disturbance, i.e. the open-loop control, or a feedback system, i.e. the closed-loop control. Most of previous active control techniques aimed at controlling vortex shedding. Blevins [7] explored the influence of a transverse sound wave on vortex shedding from a cylinder at a Reynolds number $Re = 2\text{–}4 \times 10^4$, based on the free-stream velocity and the characteristic height of the cylinder. The acoustic

*Corresponding author. Tel.: +852 2766 6769; fax: +852 2365 4703.
E-mail address: mmlcheng@polyu.edu.hk (L. Cheng).

0022-460X/$ - see front matter © 2007 Elsevier Ltd. All rights reserved.
doi:10.1016/j.jsv.2007.10.011

wave was emitted from two loudspeakers mounted on the two sides of a wind tunnel test section. It was found that the sound introduced could increase the coherence of vortices along the cylinder axis and cause vortex shedding to be locked on with the excitation acoustic wave. Inspired by this work, Roussopoulos [8] and Ffowcs-Williams and Zhao [9] used a closed-loop method with the feedback signal from a hot wire to drive loudspeakers. The acoustic excitation from the loudspeakers suppressed vortex shedding from a cylinder at $Re = 120$ and 400, respectively. Another approach is to control the rollup motion of shear layers separated from a cylinder by oscillating or rotating the cylinder. Using this technique, Warui and Fujisawa [10] and Tokumaru and Dimotakis [11] effectively reduced the vortex strength using electromagnetic actuators. The actuators were mounted at both ends of a circular cylinder to create a cylinder motion and controlled by a feedback signal from a hot wire placed in the wake ($Re \approx 10^4$). Williams et al. [12] introduced both symmetrical and anti-symmetrical forcing into a cylinder wake ($Re = 470$) at a frequency of about twice the vortex shedding frequency (f_s) through two rows of holes located at $\pm 45^\circ$, respectively, away from the forward stagnation line of the cylinder. They managed to modify f_s and the vortex street. Baz and Kim [13] and Tani et al. [14] used piezo-ceramic actuators installed inside a cantilevered cylinder to exert a force on the cylinder. The actuators were excited by a feedback signal measured from the structural vibration, thus increasing the damping of the cylinder and effectively reducing the structural vibration at the occurrence of resonance ($Re = 17{,}160$–$26{,}555$), when f_s coincided with the natural frequency, f'_n, of the flow–structure system.

Cheng et al. [15] proposed a new technique by creating a local perturbation on one surface of a square cylinder in a cross flow using piezo-ceramic actuators. They demonstrated that this perturbation could manipulate fluid–structure interactions, suppressing (or enhancing) vortex shedding and/or flow-induced structural vibration, and even reducing noise. Both open- and closed-loop control have been investigated. In this review, we will focus on this technique and its development, summarizing the technique itself, applications, performances and physical mechanisms. The technique is first introduced in Section 2. Various applications based on this technique are then given in Section 3, and mechanisms behind the control are discussed in Section 4. A brief summary is given in Section 5.

2. Perturbation technique and implementation

2.1. Underlying principles

The Kármán vortex street behind a bluff body is unstable and depends on its initial conditions [16]. Local perturbations into flow, if small enough to comply with linear theory, may grow exponentially [17], exerting a significant influence on the highly nonlinear unsteady Kármán vortex street [12,18,19]. Den Hartog [20] and Parker [21] introduced small local perturbation to flow by oscillating a cylinder transversely and emitting acoustic waves inside the cylinder, respectively. Both techniques led to the enhancement of vortex shedding. The observations further imply that local perturbations may significantly influence the nature of fluid–structure interaction or the vortex-induced structural vibration. Based on this, a novel perturbation technique is conceived to provide a possible control of both flow and structural vibration. The local perturbation is imposed on the structural surface using piezo-electric actuators.

2.2. Actuation mechanism

A surface-perturbation-based control technique has been developed and local perturbation imposed on the structural surface is produced using a new type of advanced piezo-ceramic actuators, called THUNDER (THin layer composite UNimorph piezoelectric Driver and sEnsoR), developed by NASA Langley Research Center. To our knowledge, this actuator has so far been used for vibration isolation [22], aeroelastic response control [23], and active noise control [24]. Due to a special fabrication process [25], this type of actuators may produce a displacement larger than conventional piezo-ceramic actuators with acceptable load-bearing capacity. THUNDER is a multi-layer composite in which individual materials with different thermal expansion coefficients are layered on top of each other to form a "sandwich", comprising a metal base layer, a piezo-electric layer at the middle and an aluminum foil on the top; an ultrahigh performance hot-melt adhesive, LaRC^{TM}-SI, is applied between the layers. After several precise pressure and temperature cycles,

these layers are bonded together, resulting in a finished product with the characteristics of bend or curvature (Fig. 1(a)). With a voltage applied, the actuator deforms out of plane (Fig. 1(b)). Specifically, the THUNDER actuators presently used can vibrate at a maximum displacement of about 2 mm within a frequency range up to 2 kHz in the absence of loading.

2.3. Implementation of the technique

Fig. 2 presents schematically the typical implementation of the technique in the case of a rectangular cross-section bluff body in cross flow. Three THUNDER actuators are embedded in series in a slot on one side of

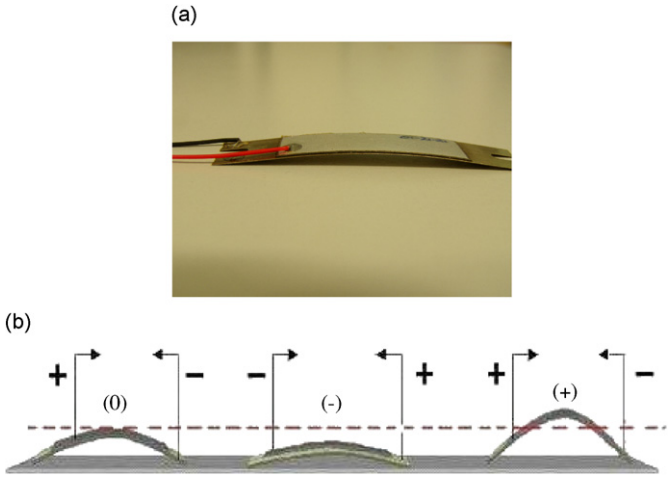

Fig. 1. Description of THUNDER actuators: (a) photo of THUNDER and (b) working principle of THUNDER: deformation vs. applied voltage.

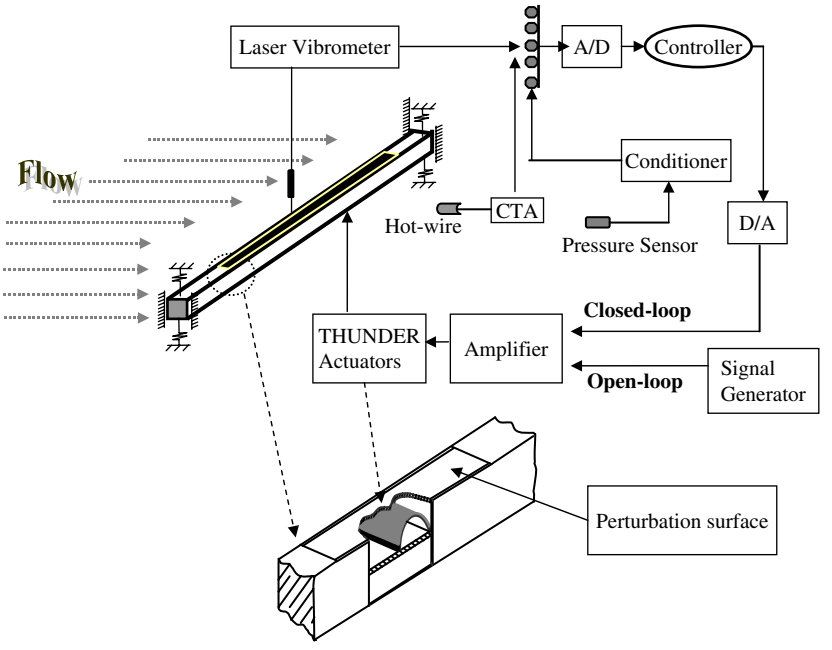

Fig. 2. Implementation of the perturbation-based control technique: schematic of mechanical configuration.

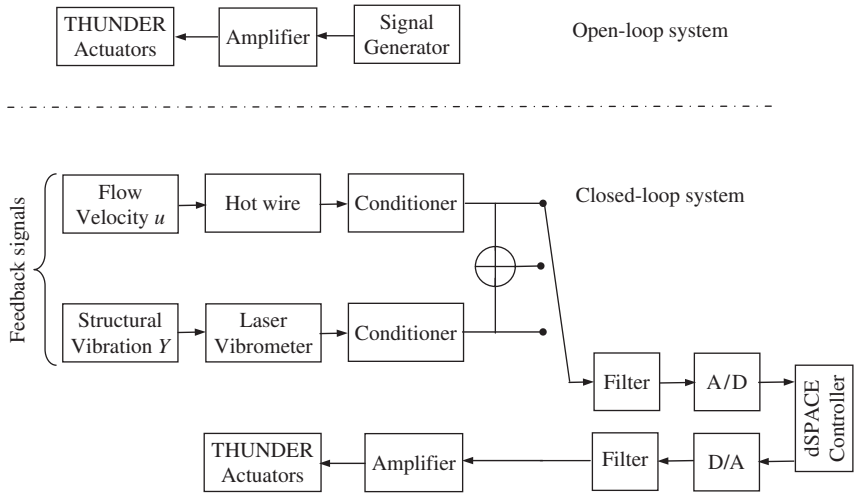

Fig. 3. Schematic of control system.

the cylinder to support a thin plastic plate, which is installed flush with the cylinder surface. One end of each actuator is adhesive-tape-fixed on the bottom side of the slot, while the other is free. The actuators and the walls of the slot around the actuators are well lubricated to minimize contact friction. Driven by the actuators, this plate will oscillate to create a local perturbation on one cylinder surface. Tests were performed to ensure the two-dimensionality of the perturbation; a very uniform motion was observed along the spanwise direction of the structure.

Both open- and closed-loop control methods may be deployed, as shown schematically in Fig. 2. For the open-loop, the actuators are simultaneously activated by a signal with controllable frequency and voltage, i.e. the perturbation frequency f_p and the perturbation voltage, generated by a signal generator. For the closed-loop, they are activated by feedback signals taken from the system. The feedback control system may take instantaneous signals from individual lateral structural vibration $\dot{Y}$ measured using a laser vibrometer or streamwise fluctuating flow velocity u measured with a single hotwire, or a combined of Y and u for feedback signals, referred to as one-element and two-element control schemes, respectively (Fig. 3). After amplification, the feedback signals are filtered and then sampled into a digital controller implemented on a dSPACE control platform for real-time data processing. The output signals from the controller are filtered and amplified again before being used to drive the THUNDER actuators. For each control scheme, the target is to minimize simultaneously Y and u, which is achieved by manually tuning the parameters of the controller. In the present work, a digital proportional-integral-derivative (PID) controller is used. The output of the controller is proportional to the input, its integral and its derivative. The design of a PID controller involves optimally setting three proportionalities, i.e. proportional gain (P), integral gain (I) and derivative gain (D) to achieve a maximum reduction in the physical parameters to be controlled. The parameter tuning process usually involves several iterations to reach the final optimal configuration. More details on controller design and tuning can be found in Ref. [26].

3. Applications

The perturbation technique has been applied to various physical systems, including (1) open- and closed-looped control of one-degree-freedom resonant fluid–structure system; (2) closed-looped control of multi-degree-freedom flexible structure; and (3) the control of vortex-induced noise. Main results are summarized in this section. Discussion on the physical mechanism of the control is given in the next section.

In the results presented hereinafter, experiments were conducted in a closed circuit wind tunnel with a square working section (0.6 m × 0.6 m) of 2.4 m in length. The wind speed of the working section is up to 50 m/s, which is controlled by a Dynagen inverter (S36-4060-686, 90 A) with a resolution of 0.3 rpm/60 Hz. The streamwise mean velocity uniformity is about 0.1% and the turbulence intensity is less than 0.4%.

Advanced flow and structural vibration diagnostic techniques such as particle image velocimetry (PIV), laser Doppler anemometer (LDA), laser vibrometer, and hotwires, are used.

3.1. Case 1: Control of a one-degree-of-freedom resonant fluid–structure system

The perturbation technique was first applied to the open-loop control of a resonant fluid–structure system, where the vortex shedding frequency f_s was synchronized with the natural frequency f_n' of an oscillating square cylinder [15]. The cylinder, flexibly supported at both ends, was allowed to vibrate only in the lift direction. Three actuators, having a dimension of 63.3 mm × 13.8 mm × 0.2 mm and a dome height of 3.84 mm were connected in series and embedded underneath one side of the cylinder and parallel to the flow. Before installation, each actuator was individually calibrated, showing very consistent characteristics in terms of amplitude and phase lag. Once installed, these actuators were simultaneously activated by a sinusoidal wave, thus forcing the cylinder surface to oscillate. Under the resonance condition, the oscillating surface reached 0.42 mm in amplitude, or 2.8% of the cylinder height h. Measurement using the laser vibrometer at different spanwise locations showed a uniform oscillation of the surface. It was observed that, as the normalized perturbation frequency f_p^* (asterisk denotes the normalization of f_p, by the cylinder height h, and the free-stream velocity U_∞; $f_p^* = f_p h/U_\infty$) was lower than the possible synchronization range ($0.8f_s$–$2f_s$) [27], i.e. $f_p^* = 0.11-0.26$, structural vibration (Y), vortex circulation (Γ) and mean drag coefficient ($\bar{C}_D$) were reduced to different extent. Best result was obtained in the vicinity of $f_p^* = 0.1$. At $f_p^* = 0.1$, Y, Γ, and $\bar{C}_D$ were reduced by up to 75%, 50%, and 21%, respectively. On the other hand, as f_p^* fell within the synchronization range, both Γ and $\bar{C}_D$ were increased; at $f_p^* = 0.13$, Γ was doubled and $\bar{C}_D$ grew by 35%.

The open-loop control suffered from two major drawbacks. First, the effective frequency range to achieve the desired performance was relatively narrow. Second, the energy required to drive the actuators was rather high. To resolve the problems, the closed-loop control method was introduced [26]. Two one-element control schemes and one two-element control scheme were deployed, where the feedback signal was structural vibration Y (Y_control scheme), fluctuating flow velocity u (u_control scheme), and a combination of both (u+Y_control scheme), respectively. The Y_control scheme or u_control scheme did not necessarily perform better than the open-loop control. However, the u+Y_control led to the almost completely destroyed Kármán vortex street and to an 82% reduction in Y, 65% in Γ, and 35% in $\bar{C}_D$, greatly outperforming the open-loop control. The u+Y_control is compared with the open-loop control ($f_p^* = 0.1$) in terms of the control effect on structural vibration (Fig. 4) and flow (Fig. 5). There is a drastic reduction in the structural vibration once the controller is on, especially in the case of the closed-looped control. Corresponding changes in flow are evident

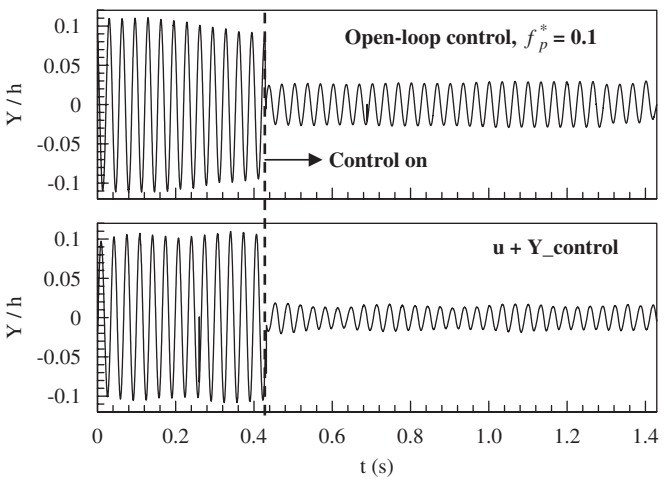

Fig. 4. Control effect on structural vibration Y for one-degree-freedom cylinder.

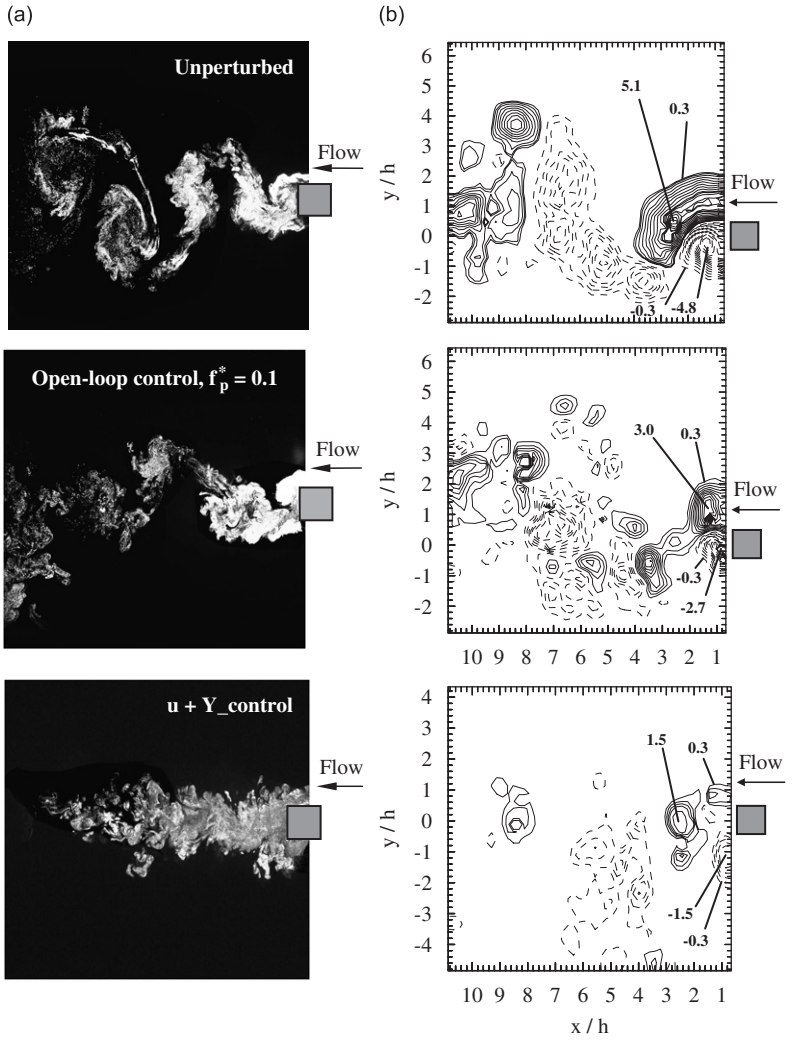

Fig. 5. Control effect on flow for one-degree-freedom cylinder. (a) Typical laser-induced fluorescence (LIF) flow visualization and (b) PIV measured iso-contours of spanwise velocity.

(Fig. 5a). With the deployment of the close-looped control, the vortex street in the absence of control completely disappears. Fig. 5(b) presents the iso-contours of the normalized spanwise vorticity, $\omega_z^* = \omega_z h/U_\infty$, from the PIV measurement, which provide quantitative information on the performance of different control schemes, thus complementing flow visualization results. The control results of one-element schemes were not as good as two-element scheme (not shown), suggesting that the proper choice of the feedback signal is crucial.

The decreased Y was attributed to the modification of the fluid–structure system damping ratio ζ_e, defined as the sum of structural damping (ζ_s) and fluid damping (ζ_f). Fig. 6 presents ζ_e under different control schemes, calculated using an auto-regressive moving average (ARMA) technique from the time series of Y [28]. The ARMA model with an order of 190 and 70,000 data points were used for calculation. Without perturbation, vortex shedding synchronizes with structural vibration, and ζ_e was less than ζ_s, albeit slightly, suggesting a negative ζ_f since $\zeta_e = \zeta_s + \zeta_f$. The negative ζ_f simply means that vortex shedding enhances the structural vibration. For the open-loop control, ζ_e increases by 163.2%, compared with the unperturbed. Similarly, the closed-loop control using the Y_control, u_control, and u+Y_control leads to an increase in ζ_e by 37.9%, 97.7%, and 271.4%, respectively, resulting in effective reduction in Y.

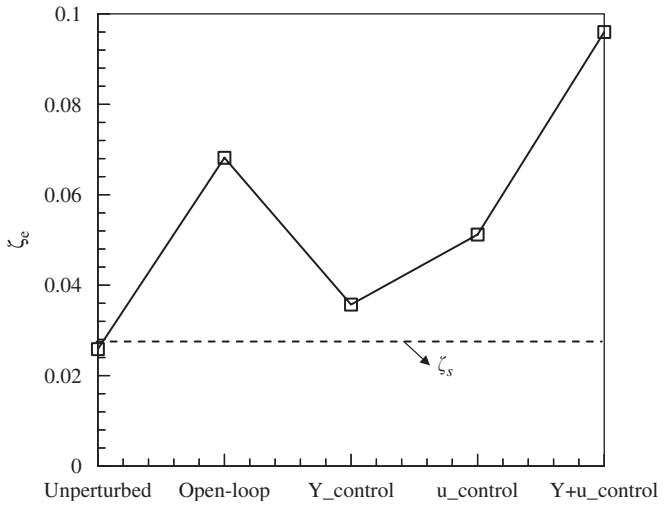

Fig. 6. Effect of open- and closed-loop control on fluid–structure system damping ratios, ζ_e. The dash line denotes the structural damping ratio ζ_s measured without flow.

3.2. Case 2: Control of multiple-degree-of-freedom system

The perturbation-based control technique was applied to control the fluid–structure interaction on a multi-freedom flexible structure. Most of the previous investigations targeted on rigid cylinders on flexible supports and neglected the flexural nature of an engineering structure, which implies multiple degrees of freedom when vibrating. In practice, however, engineering structures are frequently flexible. Problems related to fatigue or noise radiation are mainly related to the flexural vibration of these structures, especially at the occurrence of resonances, when the vortex shedding frequency coincided with one of the natural frequencies of the system. In some cases, the higher modes of structural vibration can be far more violent than the first-mode vibration. In practice, the occurrence of resonances can be avoided in a reasonable design of engineering structures; for instance, this may be achieved, under a given flow condition, by properly choosing structure parameters relating to its mass and stiffness, which determine the natural frequencies of the structure. As such, most engineering structures are operated under non-resonant conditions, which can be persistent and excessive. As a matter of fact, in the context of flow-induced vibrations, the non-resonance vibration can have amplitude well exceeding that of the first mode resonance given a considerably higher reduced velocity. Therefore, the non-resonance vibration can have a significant impact on the fatigue life of engineering structures in the long run. From the control point of view, non-resonant cases are far more challenging, compared with resonant ones. For example, vibrations at resonance are mostly dominated by one mode, but the non-resonant vibrations of engineering structures in general involve responses from various modes, resulting to a great extent in the increased degree of difficulty in control.

Closed-loop control was performed for a flexible square cylinder with fixed supports at both ends under resonance [29] and non-resonance conditions [30], respectively. Different control schemes were investigated based on the feedback signals from either individual or combined responses of structural vibration Y and u. Under resonance, f_s coincided with the first-mode natural frequency of the fluid–structure system. The results are tabulated in Table 1. Both resonant and non-resonant flexural vibration of a flexible cylinder can be effectively controlled using the present perturbation technique. Spectral analysis showed a systematic reduction in amplitude at all major frequencies, namely the first resonance frequency and its harmonics in the resonance case, and the first and third natural frequencies as well as the vortex shedding frequencies and their higher harmonics (not shown). Again, a suitable choice of the feedback signal is crucial in determining the effectiveness of the control (Table 1). The control performances in terms of suppressing structural vibration are gradually improved following the sequence of u_, Y_, and u+Y_Control. The two-element schemes again

Table 1
Control performances of various control schemes for different control cases

Control target	Fix supported flexible cylinder (resonance)			Fix supported flexible cylinder (non-resonance)	
Scheme variable[a]	u_control	Y_control	u+Y_control	Y_control	u+Y_ control
Y_{rms}	24%↓	47%↓	71%↓	37%↓	58%↓
$A_{y,\mathrm{rms}}$	25%↓	40%↓	65%↓	31%↓	52%↓
u_{rms}	37%↓	36%↓	63%↓	36%↓	53%↓
Γ	47%↓	54%↓	85%↓	54%↓	88%↓
$\bar{C}_D$			30%↓		
$V_{p,\mathrm{rms}}$	106 Volts	80 Volts	54 Volts	75 volts	55 volts

[a] Y_{rms}: rms value of the cylinder displacement, $\varepsilon_{y,\mathrm{rms}}$: rms value of the cylinder strain; u_{rms}: rms value of the fluctuating flow velocity; Γ: vortex circulation; $\bar{C}_D$: mean drag coefficient; $V_{p,\mathrm{rms}}$: rms value of the perturbation voltage.

perform much better than the one-element scheme, in terms of suppressing both vortex shedding and structural vibration. Similar analyses on system damping as those conducted in Section 3.1 confirmed that the increase in the control performance is attributable to an effective increase of system damping at all major resonance frequencies. It is pertinent to note that, apart from its higher performance, the input energy required by the two-element schemes is minimal. It is the combination of Y and u signals, not individual Y or u, that contains the information on fluid–structure interactions and thus warrants the best performance.

3.3. Case 3: Control of vortex-induced noise

Vortex-induced noise is another type of problems associated with flow separation from a structure. Depending on the excitation source or the separated flow, flow-induced noise can be classified into two categories, i.e. impinging and non-impinging cases, where noise is generated by the impingement of vortices from the upstream on a downstream hard surface, and by vortex shedding from a bluff body, respectively. Both will be discussed in this section.

The perturbation-based control technique was first applied to control the blade–vortex interaction (BVI) and to suppress the BVI noises. When a hard-surfaced body such as blade, foil, wedge or fin is subjected to an oncoming vortical flow, incident vortices may be distorted so rapidly that a sharp pressure rise is induced at the leading edge of the body [31–33]. This pressure rise in turn causes the generation of an intense impulsive sound and subsequent radiation to the far field. Fig. 7(a) shows the set-up used in experiments, in which a circular cylinder was used as the vortex generator and a NACA0012 airfoil was placed downstream. Piezo-ceramic actuators were installed near the leading edge of the airfoil. Considering difficulties in measuring directly the BVI noise, the origin of the noise, i.e. the fluctuating flow pressure p at the leading edge of the airfoil, was used as the control target [34].

Two closed-loop control schemes were examined, deploying p and u near the airfoil leading edge as the feedback signal, respectively. Experimental results indicated that the control scheme based on u led to 40% impairment in Γ of oncoming vortices and a simultaneous reduction in p by 39%, outperforming the control scheme based on p. The overall performances of the closed-loop control schemes in various control cases are summarized and compared in Table 2. Note that the input energy E, approximately given by $E = 2\pi f_s C_e V_p^2$ [35], to actuators is a good criterion for quantifying the control efficiency of various control schemes. Here C_e and V_p stand for the total capacitance of the actuators and the perturbation voltage exerted on the actuators, respectively. The results demonstrate unequivocally the effectiveness of the control technique. The u_control, with lower E, outperforms P_control in terms of both control performances and efficiency probably because u reflects the excitation source of fluid–structure interaction.

The non-impinging case was examined using the set-up shown in Fig. 7(b). Experiments were carried out in a closed circuit wind tunnel, which was specially designed for aero-acoustic testing with a low level

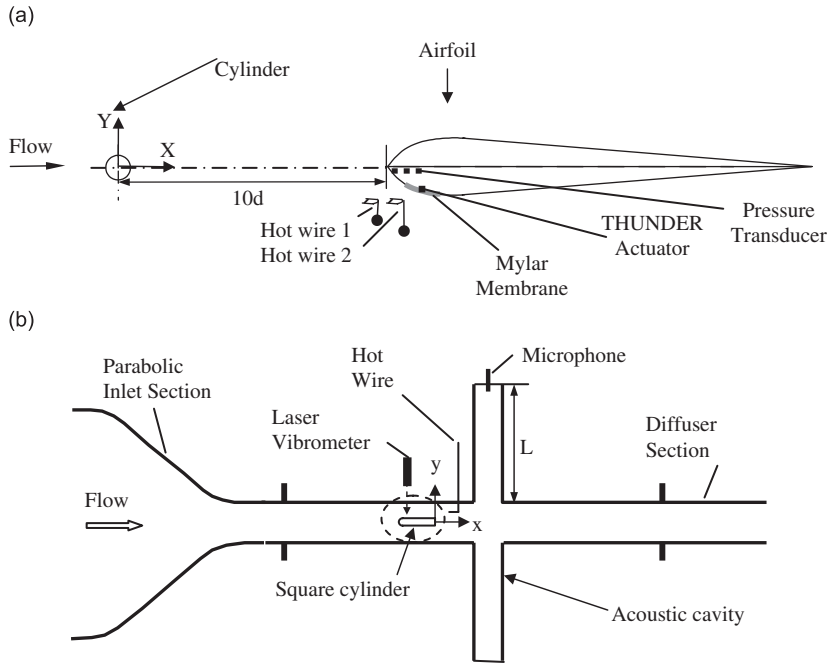

Fig. 7. Control of vortex-induced noise: (a) Blade–vortex interaction and (b) vortex-induced acoustic resonance.

Table 2
Control performances of blade–vortex interaction

Variables	p_control	u_control
u_{rms}	18%↓	21%↓
Γ	31%↓	40%↓
P_{rms}	30%↓	39%↓
E (J)	0.037	0.016

of background noise. A square cylinder, on which actuators were installed, was used as a wake generator. Two axisymmetric cavities were installed downstream of the cylinder on the top and bottom wall of the tunnel to act as acoustic resonators. Dimensions of the cavity were initially estimated based on its first resonance frequency $f'_a \approx C/4L$, where C is the sound speed and L the depth of each cavity. Flow speed was adjusted to ensure the occurrence of the acoustic resonance within the cavity. The distance between the trailing edge of the plate and the downstream wall of the cavities was chosen to be about 9.8 h to ensure an effective fluid–acoustic interaction within the near wake of the flow field and thus strengthen the resonance.

Open-loop control was applied to reduce the sound pressure level (SPL) measured inside the acoustic cavity at f'_a when the frequency of vortex shedding from the cylinder coincides with the first resonant frequency of the cavity. Fig. 8 shows a typical power spectrum of the SPL, with and without perturbation, at $Re = 6200$. Four evident peaks appear in the SPL-spectrum in the absence of control, corresponding to the natural frequency of shear layer separation, i.e.f'^*_{SL}, the frequency of the first, third, and fifth cavity acoustic mode, i.e. $f'^*_{\mathrm{SL}}(=f^*_s)$, f''^*_a, and $f^{(5)*}_a$, respectively. Once control is introduced, the SPL at $f'^*_a = f^*_s$ retreats from 83 to 74.8 dB. A small peak emerges at $f^*_p = 0.039$ apparently due to perturbation. Reductions in the SPL at f''^*_a and $f^{(5)*}_a$ are noticeable. Similar phenomena were also noticed for some non-resonance cases (not shown). It is evident that both the vortex-induced acoustic resonance and non-resonance can be effectively controlled using the perturbation technique.

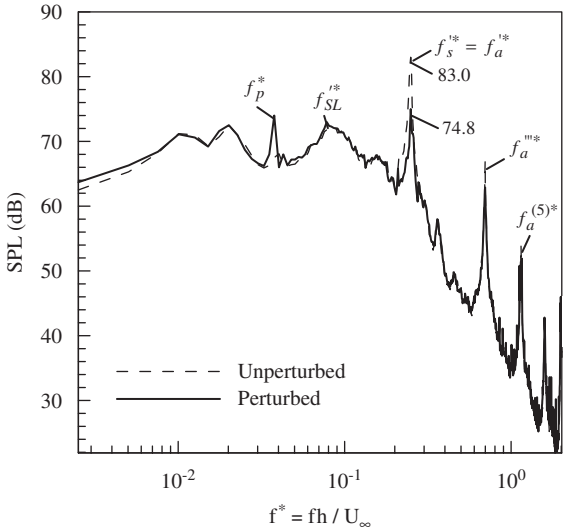

Fig. 8. Sound pressure level (SPL) inside the acoustic cavity at $Re = 6200$.

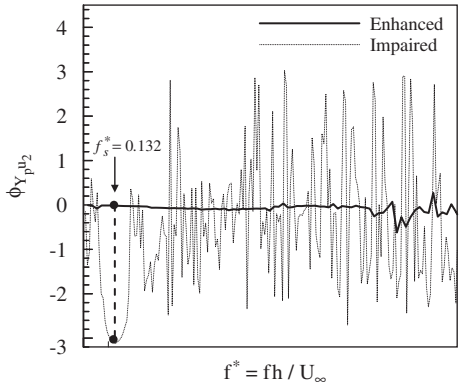

Fig. 9. Typical spectral phase $\phi_{Y_p u_2}$ between the perturbation displacement (Y_p) and the streamwise flow velocity (u_2) under control.

4. Physical mechanisms

Insight may be gained into the underlying physical mechanisms of the perturbation-based control by examining how the perturbation, flow and structure interact with each other. We first examine the closed-loop control of a stationary cylinder wake in order to separate the perturbation motion from that of cylinders. Fig. 9 shows the variation of a typical spectral phase $\phi_{Y_p u_2}$ between the perturbation displacement Y_p and the streamwise flow velocity u_2, measured at a location where the major characteristics of vortex shedding may be reflected. The spectral phase between signals α_1 and α_2 is defined as $\phi_{\alpha_1\alpha_2} \equiv \tan^{-1}(Q_{\alpha_1\alpha_2}/\mathrm{Co}_{\alpha_1\alpha_2})$, calculated using a fast Fourier transform (FFT) method [37], where $\mathrm{Co}_{\alpha_1\alpha_2}$ and $Q_{\alpha_1\alpha_2}$ stand for the cospectrum and quadrature spectrum, respectively. The control causes $\phi_{Y_p u_2}$ to be either about zero over a large frequency range or $-\pi$ over a small range of frequencies around f_s^*. Note that the vertical velocity component, v, leads u within the Karman vortex by about $\pi/2$ above the centreline [39]. This implies that the measured u_2 could be about $\pi/2$ lagging behind that of the lateral velocity (v_2) at the same point. On the other hand, given the perturbation surface oscillates harmonically, the measured Y is $\pi/2$ lagging behind the surface moving velocity $\dot{Y}$. Therefore, the phase relationship between u_2 and Y could represent that between v_2 and $\dot{Y}$. Therefore, $\phi_{Y_p u_2} = 0$ corresponds to in-phased $\dot{Y}_p$ and v_2, which promotes the roll-up motion of vortices and

subsequently the vortex strength. On the other hand, $\phi_{Y_p u_2} = -\pi$ at f_s^* corresponds to anti-phased $\dot{Y}_p$ and v_2 associated with vortex shedding, that is, the surface perturbation created by actuators move oppositely to the vortex motion in the lateral direction. The opposite or collided movement between $\dot{Y}_p$ and v_2 is responsible for the greatly impaired vortex strength behind the cylinder (Fig. 5).

From a different perspective, $\phi_{Y_p u_2}$ roughly represents the phase relation between the two components of the structural force $\mathbf{F}'_y$ on flow in the lateral direction [36], i.e. the unperturbed component $\mathbf{F}'_{y,u}$ due to the structural surface without perturbation and the perturbation component $\mathbf{F}'_{y,p}$ due to the local surface perturbation activated by the actuators. The three force vectors satisfy the relation $\mathbf{F}'_y = \mathbf{F}'_{y,u} + \mathbf{F}'_{y,p}$. Thus, $\phi_{Y_p u_2} = 0$ corresponds to in-phased $\mathbf{F}'_{y,u}$ and $\mathbf{F}'_{y,p}$, leading to an increase in $\mathbf{F}'_y$. On the other hand, $\phi_{Y_p u_2} = -\pi$ corresponds to anti-phased $\mathbf{F}'_{y,u}$ and $\mathbf{F}'_{y,p}$, resulting in a decrease in $\mathbf{F}'_y$. This provides a physical explanation about the alteration in the vortex strength. In addition, results reported in Ref. [36] also showed that similar control effects were produced as *Re* varied within a range, suggesting the control technique possessed a certain degree of adaptiveness and robustness.

The modified vortex strength by perturbation will influence interactions between flow and structure. As an example, let us examine the behaviours of ϕ_{Yu_2} in the case of a rigid cylinder flexibly supported (Fig. 10) when the resonant fluid–structure interaction is perturbed. Note that the relationship between Y and u_2 at f_s^* equivalently describes that between $\dot{Y}$ and v_2 around the structure [15]. In the absence of perturbation, ϕ_{Yu_2} is zero over a range of frequencies about f_s^*, implying that the unperturbed flow is synchronized with the cylinder oscillation. However, in the open-loop control ($f_p^* = 0.1$) or the closed-loop control such as the u+Y_control, ϕ_{Yu_2} may be altered from 0 to π over a range of frequencies around f_s^*, suggesting that the synchronizing relationship between flow and structure is significantly modified; the flow and the structure now tend to move oppositely to each other. As a consequence, both vortex shedding and structural vibration are greatly weakened. The spectral coherence $\mathrm{Coh}_{\alpha_1\alpha_2} = (\mathrm{Co}^2_{\alpha_1\alpha_2} + Q^2_{\alpha_1\alpha_2})/E_{\alpha_1}E_{\alpha_2}$ provides a measure of the degree of correlation between the Fourier components of α_1 and α_2 [37]. Under no control condition, the peak in Coh_{Yu_2} (Fig. 11) at f_s^* reaches about 0.66, suggesting a strong correlation between flow and structure, but recedes by 77% under the open-loop control ($f_p^* = 0.1$) and by 83% under the u+Y_control; the coupled relationship between flow and structure is remarkably impaired.

Based on the above analyses, an interpretation for the control mechanism of the perturbation-based control is now proposed. Vortex-induced vibration originates from fluid–structure interactions. The open- or closed-loop controlled perturbation on the structural surface may modify the nature of interaction between flow and structure, either reinforcing or weakening each other, and acting to promote or downgrade the strength of

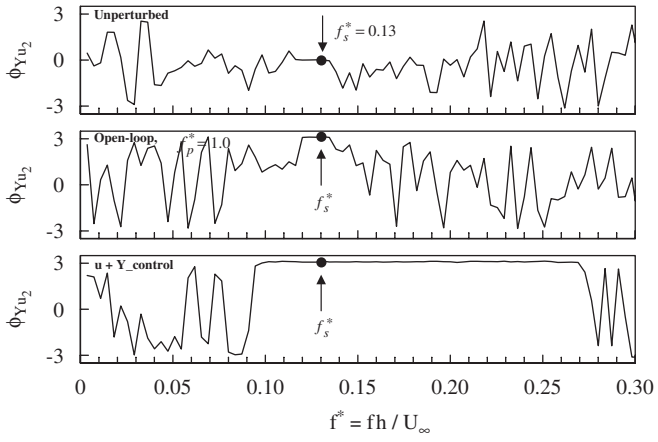

Fig. 10. Typical spectral phases ϕ_{Yu_2} between the structural vibration (Y) and the streamwise flow velocity (u_2) reflecting fluid–structure interaction with and without control.

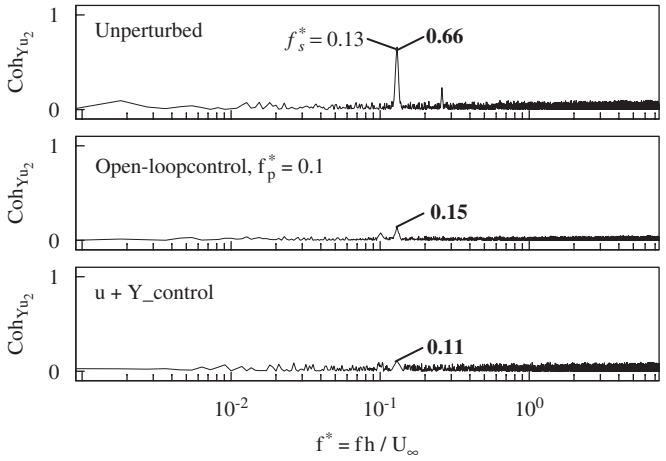

Fig. 11. Typical spectral coherences Coh_{Yu_2} between the structural vibration (Y) and the streamwise flow velocity (u_2) reflecting fluid–structure interaction with and without control.

vortical motion. Physically, this corresponds to the enhancement and impairment, respectively, of the force acting on the flow exerted by the structure.

The differences in the control performances of open- and closed-loop control schemes are attributed to different control signals, which are used to drive actuators. In the open loop, the perturbation signal is independent of flow, interactions between flow and a structure are sensitive to f_p^*. Depending on whether f_p^* is within or outside the synchronization range, the coupled fluid–structure interaction may be either enhanced or weakened. For the closed-loop control, the feedback signal is the control signal. The one-element control schemes use the signal of either structural vibration or flow velocity for the feedback signal. Among the choices of the feedback signals, the one (i.e. the flow) that contains the excitation source of fluid–structure interactions has best performances. The feedback signal in one-element schemes contains only part of the information of fluid–structure interactions. Consequently, the control performance of one-element schemes is limited. On the other hand, flow–structure interactions are well reflected in the feedback signal of the two-element schemes. For example, the $u+Y$_control utilizes a combination of flow and structural vibration as the feedback signal, which reflects the interaction/coupling between flow and structural vibration. Therefore, the two-element schemes exhibit superiority over the one-element schemes in terms of control performance and efficiency.

Vortex–airfoil interaction differs from flow-induced vibration in that the airfoil leading edge is bombarded by incident vortices, instead of shedding vortices. The investigation of the relationship between flow and perturbation showed that the spectral phase $\phi_{\dot{Y}_p v}$ between the lateral fluctuating flow velocity v and the airfoil surface perturbation velocity $\dot{Y}_p$ (approximately in the lateral direction) at f_s^* (not shown) was close to $-\pi$ for both p_ and u_control schemes [34], implying the opposite or collided movements between the local airfoil surface perturbation and the local vortical flow. The 'colliding effect', that is, the anti-phased v and $\dot{Y}_p$, on the local vortical flow may exert a significant influence on the whole unsteady vortex structure and subsequently weakening the vortex strength, and in turn cause a weakened fluctuating flow pressure near the airfoil leading edge and subsequently its induced BVI noise because of their close link [33,38].

The same issue may also be interpreted in terms of the force interaction between the perturbed surface and the oncoming vortical flow. To this end, the force applied by the airfoil on the flow is analyzed at the interface between the vortical flow below the airfoil leading edge and the airfoil surface. The lateral resultant force $\mathbf{F}_y$ on the flow can be rewritten as $\mathbf{F}_y = \mathbf{F}_{s,y} + \mathbf{F}_p$, where $\mathbf{F}_{s,y}$ is the y-component of the force exerted by the airfoil surface on the flow in the absence of perturbation and $\mathbf{F}_p$ is the additional force component due to the surface perturbation exerted by the actuators. $\mathbf{F}_p$ is in phase with the acceleration of the airfoil surface perturbation, which leads $\dot{Y}_p$ by $\pi/2$. On the other hand, $\mathbf{F}_y$ is in phase with the lateral acceleration, $\dot{v}$, of the flow and leads v by $\pi/2$. It may be therefore inferred that $\phi_{\dot{Y}_p v}$ in fact represents the relationship between $\mathbf{F}_p$ and $\mathbf{F}_y$. $\mathbf{F}_p$ should be relatively small in view of a very small perturbation amplitude. Therefore, the phase between $\mathbf{F}_p$ and $\mathbf{F}_y$ in

fact reflects that between $\mathbf{F}_p$ and $\mathbf{F}_{s,y}$ and $\phi_{\dot{Y}_p v} = -\pi$ at f_s^* corresponds to anti-phased $\mathbf{F}_p$ and $\mathbf{F}_{s,y}$, thus resulting in the impaired $\mathbf{F}_y$. In other words, due to the perturbation, the resultant lateral force on the local vortical flow below the airfoil leading edge is reduced. This 'collision' may act to reduce substantially the vortex strength [36], and hence the fluctuating flow pressure on the airfoil leading edge or the BVI noise.

5. Summary

This paper reviews recent progress made on the control of fluid–structure interaction based on the surface-perturbation technique, summarizing the major issues, including the implementation of the technique, different control schemes, control performances, various applications, and underlying mechanisms. Major conclusions are summarized below:

1. Both flow and its induced vibration, irrespective of the stiffness, boundary conditions or vibration mode (resonance or non-resonance) of the cylinder, or its induced BVI noise can be successfully and simultaneously controlled using the presently reviewed perturbation technique.
2. The open-loop control is sensitive to f_p^*. When f_p^* is within the fluid–structure synchronization range, the synchronization is enhanced, resulting in the increased structural oscillation, vortex shedding strength and drag coefficient. When f_p^* is outside the synchronization range, the synchronization is impaired, and these quantities are all weakened.
3. In the closed-loop control, a suitable choice of feedback signals is crucial. Two-element schemes better reflect the fluid–structure interaction than one-element schemes, thus resulting in a more pronounced reduction in the structural oscillation, vortex shedding strength and drag coefficient, yet less energy requirement.
4. The mechanism of the active control lies in a modification of the nature of fluid–structure interaction. The proposed perturbation technique turns the in-phased flow and structural vibration or fluctuating flow pressure into anti-phased and subsequently their correlation is diminished. This phenomenon occurs at all dominant frequencies. The inter-relationship between the perturbation-related force ($\mathbf{F}_p$) and the flow-related force ($\mathbf{F}_f$) is crucial. Anti-phased $\mathbf{F}_p$ and $\mathbf{F}_f$ leads to an effective reduction in the structural oscillation, vortex shedding strength, drag coefficient, and fluctuating flow pressure. In-phased $\mathbf{F}_p$ and $\mathbf{F}_f$ re-enforce each other, which significantly enhances these quantities.
5. The presently reviewed control technique shows certain degree of robustness, which, tuned under one *Re*, has been demonstrated to be effective over a range of *Re*.

While the technique is demonstrated to be effective in controlling fluid–structure interactions, future investigations are warranted for further improvement in the following aspects. (1) The THUNDER actuators need to be installed meticulously in order to ensure the optimum performance. Due to its working principles, its size should be adequately large to provide reasonably curved shape and to generate required displacement, which may limit its use in some applications (e.g. the control of high Reynolds number boundary layers). Other types of actuators should be explored to provide the required perturbation. (2) So far a simple PID controller has been used to assess the feasibility of the technique. More advanced adaptive algorithms, robust and with energy consumption consideration, could certainly help make the control more effective for much wider applications. (3) While providing guidance for the better design of controllers, numerical modelling and associated data analyses may complement experimental investigations, reviewed in this paper, in improving our understanding of underlying physics. Finally, there is certainly a plenty of room for the technique to be applied to a large variety of other applications such as boundary layer control, jet control, and aero-acoustic noise suppression.

Acknowledgements

The work reported in this paper was supported by Research Grants Council of Hong Kong Special Administrative Region, China (Project no. PolyU 5132/07E). The first author also wishes to acknowledge the support from a special fund for recently promoted Chair Professors given by the Hong Kong Polytechnic University. Dr. M.M. Zhang's contribution to experimental work is greatly appreciated.

References

[1] H. Schlichting, *Boundary-layer Theory*, McGraw-Hill, New York, 1979.
[2] O.M. Griffin, S.E. Ramberg, On vortex strength and drag in bluff-body wakes, *Journal of Fluid Mechanics* 69 (1975) 721–728.
[3] T. Sarpkaya, Vortex-induced oscillations-a selected review, *Journal of Applied Mechanics* 46 (1979) 241–258.
[4] M.S. Howe, *Acoustics of Fluid– Structure Interactions*, Cambridge University Press, Cambridge, UK, 1998.
[5] M.M. Zdravkovich, Review and classification of various aerodynamic and hydrodynamic means for suppressing vortex shedding, *Journal of Wind Engineering and Industrial Aerodynamics* 7 (1981) 145–189.
[6] J.C. Owen, P.W. Bearman, A.A. Szewczyk, Passive control of viv with drag reduction, *Journal of Fluids and Structures* 15 (2001) 597–605.
[7] R.D. Blevins, The effect of sound on vortex shedding from cylinders, *Journal of Fluid Mechanics* 161 (1985) 217–237.
[8] K. Roussopoulos, Feedback control of vortex shedding at low Reynolds numbers, *Journal of Fluid Mechanics* 248 (1993) 267–296.
[9] J.E. Ffowcs-Williams, B.C. Zhao, The active control of vortex shedding, *Journal of Fluids and Structures* 3 (1989) 115–122.
[10] H.M. Warui, N. Fujisawa, Feedback control of vortex shedding from a circular cylinder by cross-flow cylinder oscillations, *Experiments in Fluids* 21 (1996) 49–56.
[11] P.T. Tokumaru, P.E. Dimotakis, Rotary oscillation control of a cylinder wake, *Journal of Fluid Mechanics* 224 (1991) 77–90.
[12] D.R. Williams, H. Mansy, C. Amato, The response and symmetry properties of a cylinder wake subjected to localized surface excitation, *Journal of Fluid Mechanics* 234 (1992) 71–96.
[13] A. Baz, M. Kim, Active modal control of vortex-induced vibrations of a flexible cylinder, *Journal of Sound and Vibration* 165 (1993) 69–84.
[14] J. Tani, J. Qiu, Y. Liu, Robust control of vortex-induced vibration of a rigid cylinder supported by an elastic beam using μ-synthesis, *Journal of Fluids and Structures* 13 (1999) 865–875.
[15] L. Cheng, Y. Zhou, M.M. Zhang, Perturbed interaction between vortex shedding and induced vibration, *Journal of Fluids and Structures* 17 (2003) 887–901.
[16] P.W. Bearman, On vortex street wakes, *Journal of Fluid Mechanics* 28 (1967) 625–641.
[17] M. Provansal, C. Mathis, L. Boyer, Benard–von Kármán instability: transient and forced regimes, *Journal of Fluid Mechanics* 182 (1987) 1–22.
[18] F.B. Hsiao, J.Y. Shyu, Influence of internal acoustic excitation upon flow passing a circular cylinder, *Journal of Fluids and Structures* 5 (1991) 427–442.
[19] X.Y. Huang, Feedback control of vortex shedding from a circular cylinder, *Experiments in Fluids* 20 (1996) 218–224.
[20] J.P. Den Hartog, *Mechanical Vibrations*, McGraw-Hill, New York, 1947.
[21] R. Parker, Resonance effects in vortex shedding from parallel plates, some experimental observations, *Journal of Sound and Vibration* 4 (1966) 62–72.
[22] J.P. Marouzé, L. Cheng, A feasibility study of active vibration isolation using THUNDER actuators, *Smart Materials and Structures* 11 (2002) 854–862.
[23] J.L. Pinkerton, R.W. Moses, A feasibility study to control airfoil shape using THUNDER, *NASA Technical Memorandum 4767*, 1997.
[24] V. Jayachandran, N.E. Meyer, M.A. Westervelt, J.Q. Sun, Piezoelectrically driven speakers for active aircraft interior noise suppression, *Applied Acoustics* 57 (1999) 263–277.
[25] B.M. Copeland, J.D. Buckley, R.G. Bryant, R.L. Fox, R.F. Hellbaum, THUNDER—an ultra-high displacement piezoelectric actuator, NASA Langley Research Center. Hampton, VA, 1999.
[26] M.M. Zhang, L. Cheng, Y. Zhou, Closed- loop-controlled vortex shedding from a flexibly supported square cylinder under different schemes, *Physics of Fluids* 16 (2004) 1439–1448.
[27] B.H.L. Gowda, Some measurements on the phenomenon of vortex shedding and induced vibrations of circular cylinders, *Deutsche Luft- und Raumfahrt Forschungsbericht*, No. 75-01, 1975.
[28] Y. Zhou, Z.J. Wang, S.J. Xu, W. Jin, Free vibrations of two side-by-side cylinders in a cross flow, *Journal of Fluid Mechanics* 443 (2001) 197–229.
[29] L. Cheng, Y. Zhou, M.M. Zhang, Controlled vortex-induced vibration on a fix-supported flexible cylinder in crossflow, *Journal of Sound and Vibration* 292 (2006) 279–299.
[30] M.M. Zhang, L. Cheng, Y. Zhou, Control of vortex-induced non-resonance vibration using piezo-ceramic actuators embedded in a structure, *Smart Materials and Structures* 14 (2005) 1217–1226.
[31] S. Ziada, D. Rockwell, Vortex-leading-edge interaction, *Journal of Fluid Mechanics* 118 (1982) 79–107.
[32] J.C. Hardin, S.L. Lamkin, Concepts for reduction of blade/vortex interaction noise, *Journal of Aircraft* 24 (1987) 120–125.
[33] D. Rockwell, Vortex–body interactions, *Annual Review of Fluid Mechanics* 30 (1998) 199–229.
[34] M.M. Zhang, L. Cheng, Y. Zhou, Closed-loop controlled vortex–airfoil interactions, *Physics of Fluids* 18 (2006) 046102 (12 pages).
[35] L.K. Baxter, *Capacitive Sensors: Design and Applications*, IEEE Press, New York, 1997.
[36] M.M. Zhang, L. Cheng, Y. Zhou, Closed-loop manipulation of vortex shedding from a fixed-supported square cylinder, *Experiments in Fluids* 39 (2005) 75–85.
[37] H.J. Zhang, Y. Zhou, R.A. Antonia, Longitudinal and spanwise structures in a turbulent wake, *Physics of Fluids* 12 (2000) 2954–2964.
[38] S. Lee, Reduction of blade–vortex interaction noise through porous leading edge, *AIAA Journal* 32 (1994) 480.
[39] Y. Zhou, R.A. Antonia, A study of turbulent vortices in the wake of a cylinder, *Journal of Fluid Mechanics* 253 (1993) 643.